SAND78-0624
Unlimited Release
UC-62

Performance Testing of the General Atomic Fixed Mirror Solar Concentrator

Robert M. Workhoven
V. E. Dudley, EG&G, Inc.

Prepared by Sandia Laboratories, Albuquerque, New Mexico 87185 and Livermore, California 94550 for the United States Department of Energy under Contract AT(29-1)-789

Printed May 1978

Sandia Laboratories

Printed in the United States of America

Available from
National Technical Information Service
U. S. Department of Commerce
5285 Port Royal Road
Springfield, VA 22161

Price: Printed Copy **$4.50** ; Microfiche **$3.00**

Issued by Sandia Laboratories, operated for the United States Department of Energy by Sandia Corporation

SAND78-0624
Unlimited Release
Printed May 1978

PERFORMANCE TESTING OF THE GENERAL ATOMIC FIXED MIRROR SOLAR CONCENTRATOR

Vernon E. Dudley
EG&G, Inc.

Robert M. Workhoven
Solar Total Energy Test Facility Division 5712
Sandia Laboratories
Albuquerque, NM 87115

ABSTRACT

This report summarizes the testing which was performed on the General Atomic Fixed Mirror Solar Concentrator at the Midtemperature Solar Systems Test Facility. Test Objectives are defined, test procedures are described, and results and conclusions are given.

CONTENTS

ILLUSTRATIONS

TABLES

PERFORMANCE TESTING OF THE
GENERAL ATOMIC FIXED MIRROR SOLAR CONCENTRATOR

INTRODUCTION: The General Atomic Fixed Mirror Solar Concentrator (FMSC) was the first of a series of solar collector designs to be tested in Sandia Laboratories' Collector Module Test Facility (CMTF). This facility is operated as a part of the Department of Energy's continuing program to characterize selected collector modules for possible future system use (Reference 1). The General Atomic solar collector evaluated for this report has an expected commercial value of about $168 per square meter (February 1978 price). The design was chosen for inclusion in Sandia's Mid-temperature Solar Systems Test Facility, and a 260 m^2 field is now in operation there.

TEST OBJECTIVE: The objective of this test series was to characterize the performance of a fixed mirror, concentrating solar collector manufactured by the General Atomic Company, San Diego, CA. Peak thermal efficiency at solar noon and receiver thermal losses were evaluated at fluid temperatures from about 150 to 300^{o}C.

COLLECTOR DESCRIPTION: The basic reflector of the FMSC (Figure 1) is a concave array of long, narrow, flat mirror facets fixed on a segment of a cylindrical surface. The array of flat reflecting facets produces a narrow focal line that follows a circular path as the sun moves (see Figure 2 for geometry of the light path). Because the focal line path is on the same basic cylinder as the mirror facets, the focal line can be tracked by a movable heat-receiver assembly that rotates about the center of curvature of the reflector module. The ideal minimum image width at the focus is equal to a single mirror facet width, plus an increment caused by the subtended angle of the sun. One of the mirror facets near the center of the module is tangent to the basic cylindrical curvature of the module. The remaining mirror facets are set at different angles such that all reflect incident light to the focus point. Using the tangent facet as a reference point, the surface angle of any other individual facet is one-fourth of the included angle between that facet and the tangent reference facet (see Figure 2). See Reference 2 for a more complete description of the optical principles of the FMSC.

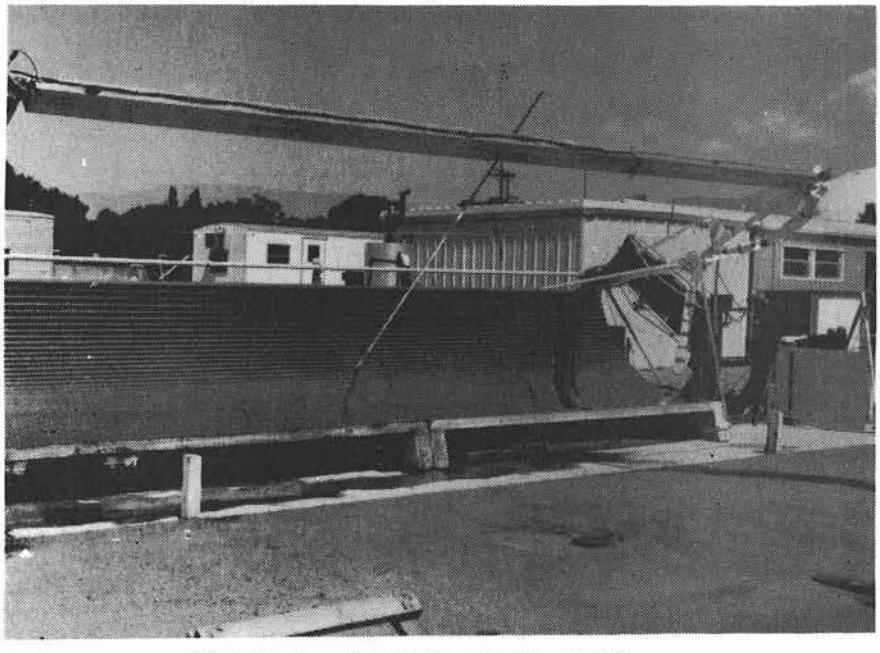

Figure 1. General Atomic FMSC

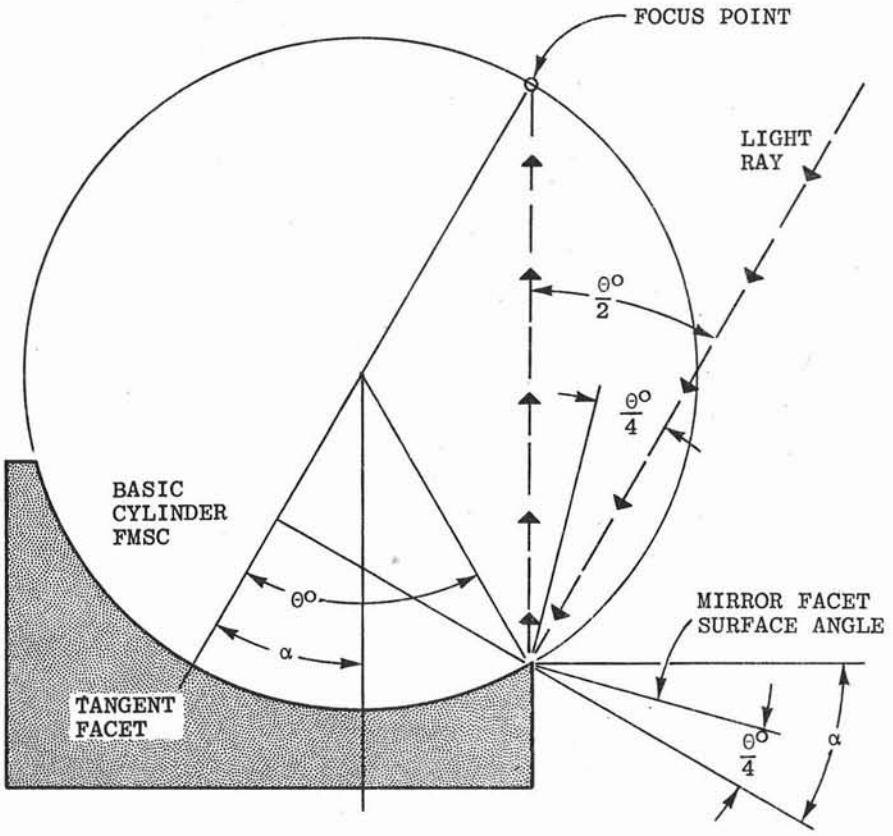

Figure 2. General Atomic FMSC Geometry.

As tested at the CMTF, the General Atomic FMSC consisted of two reinforced cast concrete modules, each 3.81 m in length with a 2.18 m aperture width (see Figure 3). Total aperture area for the two modules was 16.26 m^2. The 43 mirror facets were 5.08 cm in width; each facet length was installed as six 1.27 m long pieces. The original mirrors were made from silvered single-strength window glass about 2.4 mm in thickness. The mirror facets were arranged on a 92^o arc with a radius of curvature of 1.51 m. The mirror assembly was symmetrical about the tangent facet, and was tilted 32^o to the south to optimize heat collection characteristics at Albuquerque's latitude. The concrete modules were cast over a precision metal mold; the second-surface, silvered-glass, mirror facets were fastened to the concrete with a transferable film adhesive (3M 468) manufactured by the 3M Company.

The collector's receiver assembly moved along a circular path to track the reflector focal point; Figure 4 illustrates the movement of the receiver at different times of the year. In all positions, the receiver is aimed at the tangent mirror facet. Figure 5 is a cross-section of the receiver assembly. Primary structural support for the 7.16 m long receiver was the 10.2 cm wide aluminum channel support beam; the rectangular absorber tube and surrounding insulation were contained within the support beam. The extruded aluminum compound parabolic secondary concentrators on each side of the receiver assembly (see Figure 5) performed three

functions: 1) reconcentration of the solar energy directed at the absorber from the mirror array, 2) reduction of heat losses by being a low-grade convection barrier, 3) increased rigidity of the receiver assembly. The reflecting surface on the secondary reflectors was Kinglux, a polished anodized aluminum sheet material produced by Kingston Industries. Total hemispherical reflectivity of the Kinglux was 0.88 when new.

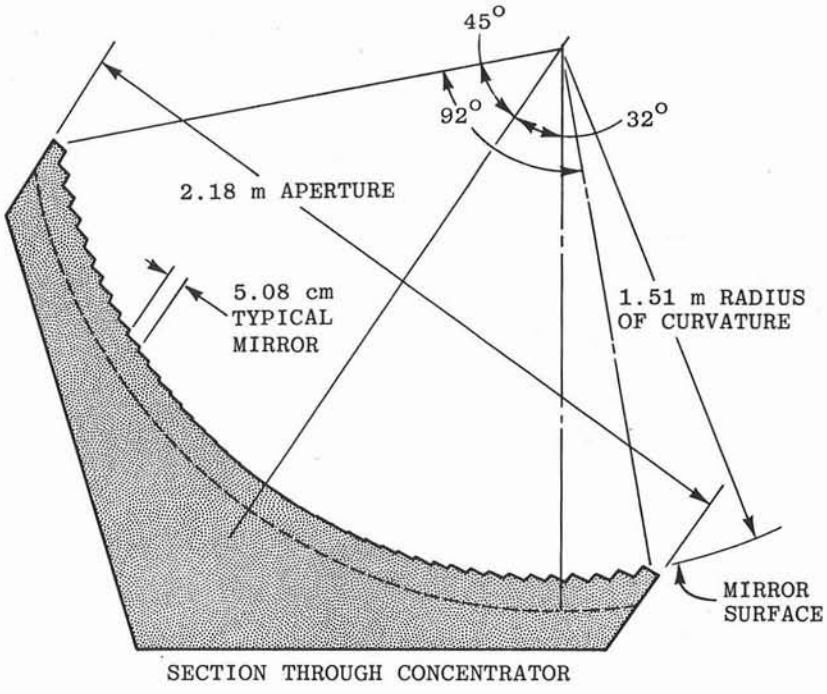

Figure 3. FMSC Dimensions.

The mild steel absorber tube was made by pressing a 3.5 cm outer diameter pipe with a 1.57 mm wall into an oval shape about 5.1 cm in width and 0.95 cm in depth. The tube had a black chrome selective coating, applied by Highland Plating Company, to enhance solar radiation absorption and reduce heat reradiation. The absorber tube mounting allowed movement from thermal expansion. The absorber tube was covered on the illuminated side by a two-mil Teflon transparent film, with a stagnant air gap between the film and the absorber tube. The back, or nonilluminated side, of the absorber tube was insulated with a form-fitted panel of Microtherm insulation manufactured in England by the Micropore Insulation Company. This material is a silica foam insulation with a much lower conductivity than other insulations, as can be seen from Figure 6 (figure extracted from Reference 3).

Data collection from the FMSC began on 16 August 1977 and was completed on 23 September 1977. Mr. G. H. Eggers and Ms. M. R. Warsicki of the General Atomic Company provided helpful advice and assistance throughout the installation and operation of the FMSC; their contribution to the success of this test series is gratefully acknowledged. Preliminary analysis of test results has been completed by General Atomic (see Reference 4).

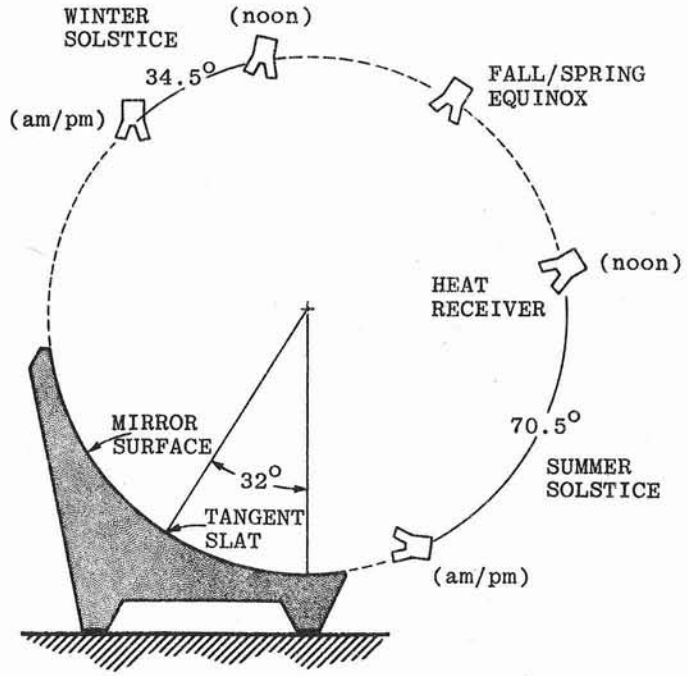

Figure 4. Annual and Daily Movement of FMSC Receiver.

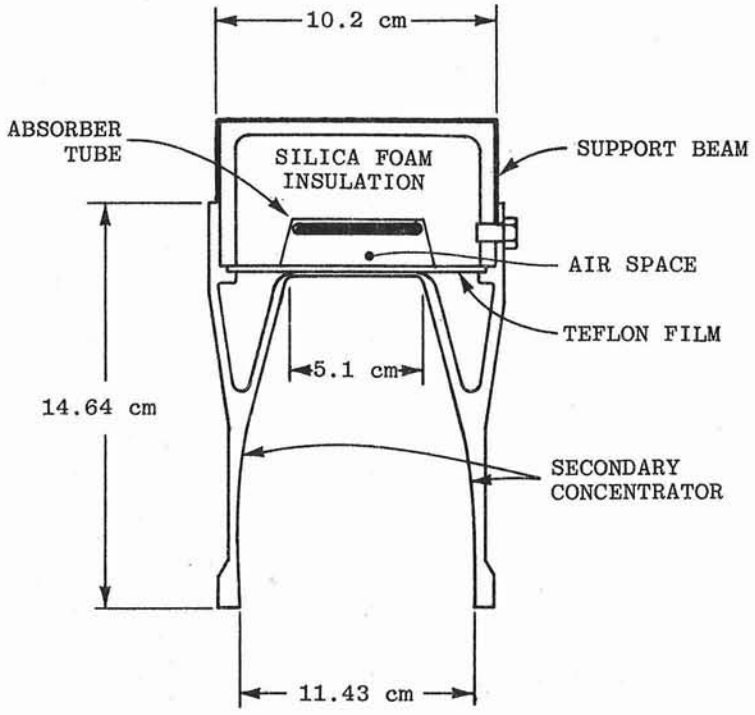

Figure 5. Heat Receiver Assembly Cross Section.

TEST FACILITY DESCRIPTION: The fluid loop used for this test series furnished a heat-transfer fluid to the collector module at input temperatures from 100°C to 300°C at flow-rates ranging from 4 to 40 liters/min. The fluid used was Therminol-66, manufactured by the Mansanto Company (see Reference 5). Other general features of the Therminol fluid test loop used for this test can be found in Reference 6.

Each day's testing began by heating the fluid loop with electric heaters to the desired collector input temperature. Usually only one temperature point was attempted in one day due to the time required for temperature stabilization and the need to conduct efficiency tests near solar noon to minimize end effects. The collector system was placed in focus as early as feasible each day so that recovered solar heat could aid in reaching the desired temperature. Temperatures below about 200°C could be attained by about 10:00 A.M. without difficulty; higher temperatures required more time due to increasing losses. The electric heaters were not large enough to heat the system to temperatures over 250°C before noon without help from the collector system. For each test, input temperature and flow-rate were maintained constant; output temperature varied according to test conditions.

The flow-rate of the Therminol-66 working fluid through the system was measured with a PRI-102A turbine flowmeter, manufactured by Flow Technology, Inc.; this flowmeter was provided by the General Atomic Company. Flow was also measured with a Ramapo SGA-101RM strain gage flowmeter. The flowmeter calibration was checked after the test series at three flow-rates by flowing fluid into a tank and plotting weight vs. time. A set of two calibrated iron-constantan thermocouples was installed at each end of the collector to determine temperatures into and out of the absorber tube. One thermocouple from each end of the absorber tube was connected as a differential pair for determining the delta temperature for calibrations of heat gain or loss. A static mixer was incorporated at each end of the absorber tube to insure thorough fluid mixing prior to measuring fluid temperature. Direct solar insolation was measured with an Eppley NIP pyrheliometer. Six locations of absorber tube skin temperature were measured with iron-constantan thermocouples welded to the outer tube surface. Ambient temperature, wind direction, and wind speed measurements completed the active data collection.

The data from the instruments described above were converted to a digital format by Doric 210 and 220 analog-to-digital data systems. An HP 2116 minicomputer processed the data and a printout was made of the data critical to the test underway.

Figure 7 is a typical printout of data obtained during an efficiency test. Figure 8 is a sample of data from a thermal loss test. In both figures, temperatures shown are in degrees Fahrenheit. Delta temperature shown is not the difference between the input and output temperatures printed; this value was obtained from the pair of differential thermocouples mentioned above. Speed of the data system was such that all data channels could be read, calculations performed, and a line in the data table printed in about 15 seconds. The average values were automatically printed after 10 data-points were accumulated. The complete data printout (as shown in Figures 7 and 8) was repeated at intervals of about 3 minutes throughout a test run. Thirty measured and calculated data values, plus 10 average

values, were available from the data system every 15 seconds. Only the data shown in Figures 7 and 8 were printed in real time. The remaining data would normally be recorded on magnetic tape for later analysis. The number of decimal places printed in Figures 7 and 8 should not be taken as an indication of data system accuracy; choice of the print format was dictated by peculiarities of the computer system used. Either a loss or an efficiency data print was made continuously; however, only those data blocks occurring under stable conditions are included in this report.

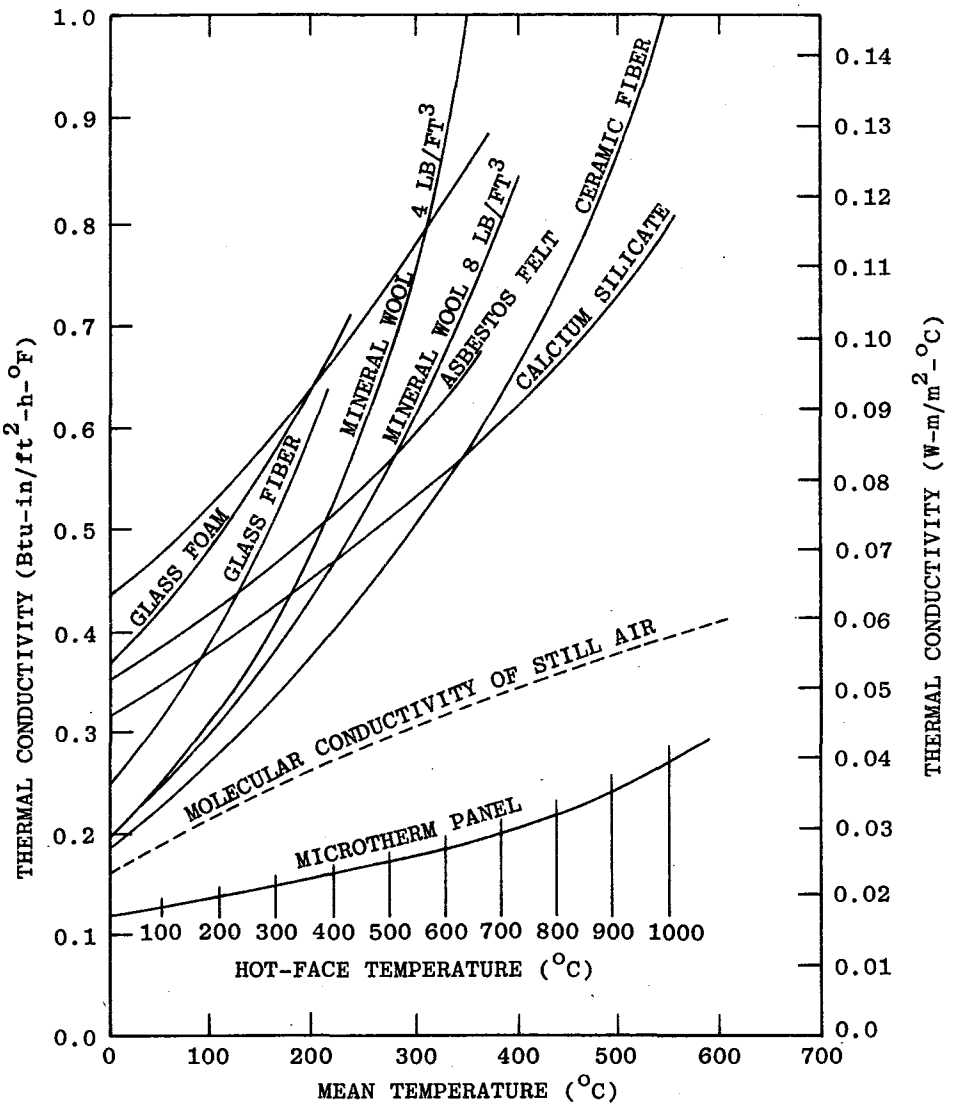

Figure 6. Thermal Conductivity Comparison of Different Insulation Materials.

GENERAL ATOMIC FIXED MIRROR COLLECTOR TEST

JULIAN DAY 238 HOUR 12 MINUTE 1 SOLAR TIME

86.2 AMBIENT TEMPERATURE (DEG F)
183 WIND DIRECTION, DEGREES
10.7 WIND SPEED, MPH

G.A. COLLECTOR TUBE SKIN TEMPERATURES
515.2 497.6 484.1 999.99 999.99 475.5

TEMP IN	TEMP OUT	SOLAR BTU/HR FT^2	DELTA TEMP	FLOW GPM	EFFICIENCY PERCENT
471.2	490.4	314.18	19.9	4.87	41.6
471.1	490.3	314.06	19.8	4.87	41.5
471.1	490.3	314.06	19.8	4.87	41.4
470.9	490.7	313.39	19.8	4.87	41.5
471.1	490.4	311.74	19.8	4.87	41.7
471.1	490.6	311.61	19.8	4.87	41.8
471.1	490.6	311.11	19.9	4.88	42.1
471.1	490.3	311.11	19.8	4.87	41.9
471	490.5	311.4	19.7	4.87	41.6
471.1	490.4	311.94	19.8	4.87	41.7
		10 POINT AVERAGES			
471.08	490.45	312.46	19.81	4.871	41.68

DIFFERENTIAL THERMOCOUPLES USED FOR DELTA T AND EFFICIENCY

END OF DATA PASS 3

Figure 7. Typical Data Printout from Efficiency Test.

GENERAL ATOMIC FMC THERMAL LOSS TEST

JULIAN DAY 238 HOUR 13 MINUTE 24 SOLAR TIME

90.1 AMBIENT TEMPERATURE (DEG F)
219 WIND DIRECTION, DEGREES
11.2 WIND SPEED, MPH

TEMP IN	TEMP OUT	FLOW GPM	DELTA TEMP	BTU/HR GAIN
467.5	465.4	4.86	-2.1	-2386.55
467.7	465.4	4.86	-2.1	-2615.5
467.7	465.4	4.86	-2.1	-2614.07
467.7	465.4	4.86	-2.1	-2615.5
467.7	465.4	4.87	-2.1	-2616.92
467.7	465.4	4.87	-2.1	-2616.92
467.7	465.3	4.86	-2	-2727.61
467.4	465.3	4.86	-2	-2385.04
467.7	465.4	4.86	-2.1	-2614.07
467.7	465.4	4.86	-2	-2615.5
	10 POINT AVERAGES			
467.65	465.38	4.862	-2.07	-2580.77

-4.7 EFFICIENCY IN PERCENT. (INCORRECT EXCEPT AT SOLAR NOON)
313.676 AVERAGE SOLAR INSOLATION, BTU/HR SQ FT

END OF DATA PASS 11

Figure 8. Typical Data Printout from Loss Test.

PERFORMANCE TEST DEFINITIONS: During a test run, specific heat and density of the Therminol-66 fluid were calculated for each data set using the average temperature of the fluid in the absorber tube and fluid properties furnished by Monsanto Industrial Chemicals Company (Reference 5). Heat gain (or loss) was then calculated from

$$Q = \dot{m}\ C_p\ \Delta T$$

where

Q = heat gain, kJ/hr
$\dot{m}$ = mass flow-rate of fluid, kg/hr
C_p = specific heat of fluid, kJ/kg^{o}C
ΔT = in/out temperature differential, ^{o}C

A successful loss measurement was one in which the values for input and output temperatures remained constant to within 0.1^{o}C or less, flow-rate varied by 0.1 liter/min or less, and delta temperature changed by 0.1^{o}C or less. Most loss test data points reported are averages of four-to-six ten-point data blocks, each block judged stable as described above, and with conditions nearly constant over the entire time averaged. Loss tests were conducted with the collector system near its normal operating position, but defocused sufficiently so that no light from the mirror would strike any part of the receiver tube assembly.

On most days, after reaching the desired temperature, loss measurements were made until about one hour before noon. Loss testing was resumed for about two hours after completion of solar noon efficiency tests; the fluid loop was then placed in a cooling mode prior to shutdown for the day.

For an efficiency test, efficiency was calculated from

$$\eta = \frac{Q/A}{I}$$

where

η = solar collector efficiency
Q = heat gain, W
A = collector aperture area, m^2
I = solar insolation, W/m^2

An efficiency measurement at a single temperature and flow-rate was usually made from about one hour before noon until about one hour after noon to ensure complete temperature and flow stabilization. This procedure ensured good definition of the peak noon efficiency.

A "good" efficiency data point consists of at least one of the ten-point averages during which input and output temperatures changed by 0.1^{o}C or less, the flow-rates varied by 0.1 liter/minute or less, the delta temperatures remained within 0.1^{o}C or less, and solar insolation remained constant to about 1%. Temperatures, flow-rate, and insolation had to have been nearly as stable as described above for at least five to ten minutes prior to the "good" data point to be

believable. Except for the continuous all-day test runs, efficiency measurements were not normally made except near solar noon, and with an insolation greater than about 950 watts/m^2. Due to the abbreviated efficiency tests with this collector, three efficiency test points are included at less than 950 W/m^2 insolation.

Prior to beginning thermal testing of the GA FMSC collector, measurements were made to determine the solar spectrum absorptance and emittance of the absorber tube's black chrome coating. The measurements were repeated after conclusion of the thermal testing.

When the thermal efficiency was determined to be significantly lower than expected, a test series was set up to measure the intensity and distribution of the light reaching the focal line. This test was accomplished by placing a water-cooled solar cell on the receiver assembly and moving the receiver slowly through the focal position. The receiver motion was calibrated to achieve a known distance per unit time. The solar cell was equipped with a slit approximately 3 mm in width to improve the position resolution.

Direct solar radiation, photocell output, and time were printed out continuously by the computer during a transit across the focal line, resulting in a reading of light intensity for approximately each 3 mm of receiver travel.

There were five positions available along the receiver length for mounting the solar cell. Since the reflector surface was made up of six mirror segments, each 1.27 m in length, it was desirable to measure the light reflected from each segment. The relationship between the five available solar cell mounting positions and the six mirror segments is shown later in this report (Figure 15). By taking the scan data at several times during the day, measurements could be accumulated for each mirror segment. Data was obtained only for the new mirrors. Analysis of the scan data was accomplished by General Atomic (Reference 4).

TEST RESULTS: Before the two FMSC modules were delivered for testing, they had been assembled and operated at the General Atomic facility in San Diego for some time. The reflecting surface was known to be deteriorating because of insufficient protective coating on the back and edges of the glass mirror facets. Initial test results confirmed that the peeling edges of the mirrors and enlarging pinholes in the silvered surface had caused significant degradation of reflectivity. Initial reflectivity of the mirrors was stated by the vendor to be about 0.92. However, later measurements showed a reflectance of only about 0.88. At the time of initial testing at Sandia, the reflectance had decreased to about 0.83. The results of these initial tests are shown in Table 1 under "Old Mirrors," and are also plotted in Figure 9; maximum efficiency achieved was 37% at 292°C output. Figure 10 shows the same efficiency data plotted as a function of average receiver fluid temperature above ambient divided by direct solar radiation.

A complete set of new mirrors was not available to dedicate to the test modules, so mirrors intended for the 260 m^2 collector field at the Midtemperature Solar Systems Test Facility were borrowed and installed over the old mirrors. The new mirrors were not glued into place, since they would shortly be needed on other collector modules. The new mirrors were made from Corning 0317 low iron glass of about 1.52 mm thickness; measured reflectivity was 0.95. Edges and backs of these mirrors were coated with a polyurethane enamel to prevent deterioration of the reflective surface.

The new mirrors provided an increase in efficiency of about 8-10% as shown in Table 1 and Figure 9, labeled "New Mirrors." This efficiency increase correlates well with the increase in mirror reflectivity from 0.82 to 0.95.

Table 1. General Atomic Peak Noon Efficiency.

Test Date	Insolation (W/m^2)	Temp Out (^oC)	Receiver Tube ΔT (^oC)	Flow Rate (liter/min)	Efficiency (%)
		Old Mirrors			
8/17/77	888	267.5	7.5	18.9	33
8/18/77	958	291.8	9.2	18.7	37
8/19/77	960	294.6	8.3	19.6	36
8/22/77	699	183.5	6.6	18.6	36
8/23/77	953	254.7	5.4	29.5	35
8/24/77	893	311.3	7.2	18.4	32
		New Mirrors			
8/25/77	987	313.7	10.2	19.2	42
8/26/77	991	255.0	9.0	18.4	43
8/29/77	938	193.1	11.3	19.3	44
		New Receiver Tube			
9/17/77	977	262.3	10.1	18.6	39
9/19/77	997	263.4	16.5	11.6	40
9/20/77	981	256.6	7.3	26.8	41
9/21/77	1031	255.8	6.7	26.7	36*

*Mylar window removed, black chrome damaged

Unfortunately, only three days of efficiency testing were completed with this collector configuration; at this point the receiver was inadvertently brought into focus without any fluid flow through the receiver. The resulting overheat and overpressure condition severely damaged the physical configuration of the absorber tube and its black chrome coating. The exact time the receiver was exposed to concentrated sunlight is not known, but was estimated to be about 20 minutes. Similarly, because the data system was not running, temperatures and pressures were not recorded. Temperatures were estimated at about 500-600^oC. Pressure was great enough to expand the oval absorber tube back to nearly its original round configuration. The absorber tube was sectioned and absorptance/emittance measured after the overheat condition (see Table 2).

Another absorber tube was available; however, its construction was not identical to the original tube. The replacement was stainless steel and had a 50% greater cross-sectional area. The wall thickness was less (only 0.71 mm vs. 1.57 mm for the original), and its black chrome coating was not the same quality (see Table 2). The replacement tube was installed on 16 September; also installed at this time was a receiver window of 1 mil Tedlar to replace the original 2 mil Teflon window, which was also damaged in the overheat incident.

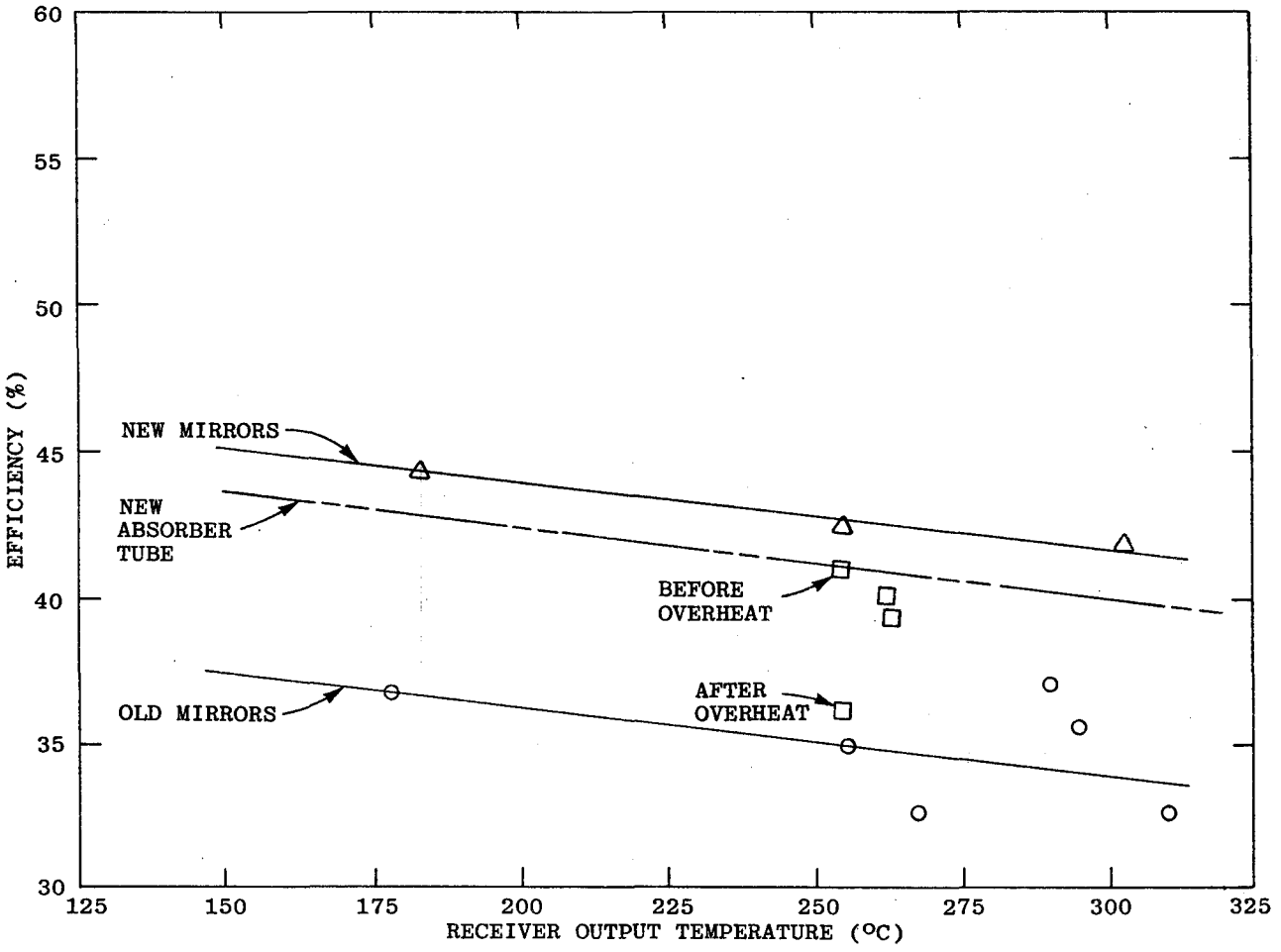

Figure 9. FMSC Efficiency.

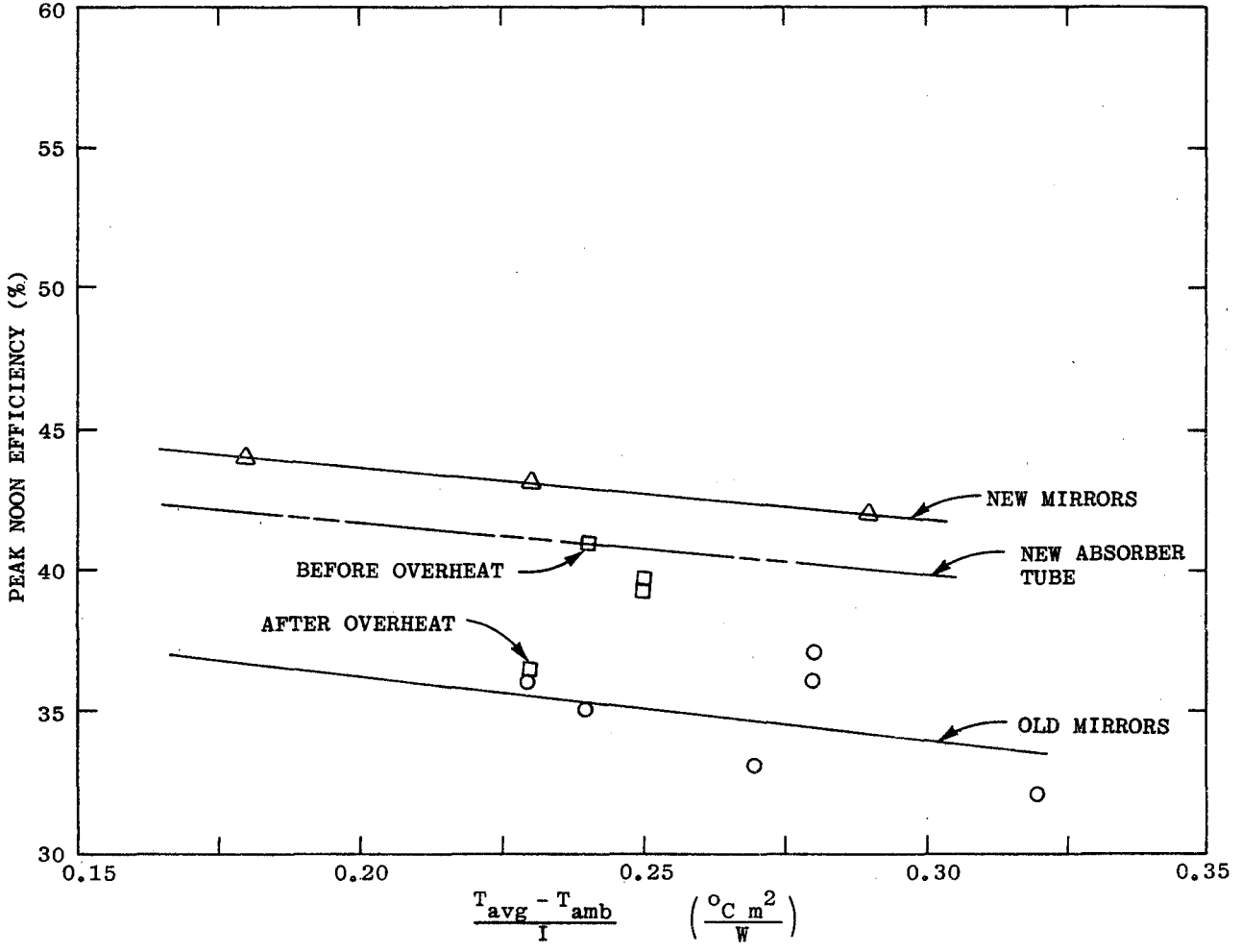

Figure 10. FMSC Efficiency.

Table 2. Absorber Tube Aborptance/Emittance.

	α		ε_{th} (300°C)	
	Before	After	Before	After
Original Tube	0.956	0.77	0.23	0.14
Replacement	0.930	--	0.10*	--

*at room temperature

The differences resulting from the new window and absorber were immediately apparent when testing was resumed--measured efficiency was about 3% lower at the same temperature and flow-rate. Efficiency was measured at three flow-rates between 11 and 27 liters/minute; an increase of about 2% was obtained between the lowest and highest flow-rates for a peak of 41% at 256°C output fluid temperature. This data is shown in Table 1 and Figure 9, labeled "New Absorber Tube." The increase of efficiency with increased flow-rates was probably due to the larger cross-sectional area of the absorber tube, causing the fluid velocity to be lower than in the original tube at the same flow-rate. Flow-rates higher than 27 liters/minute could not be attempted; the input pressure necessary for higher flow would have distorted the oval shape of the thin-walled absorber tube. The remainder of the difference in efficiency (about 1%) between the two tubes was probably due to the lower absorptance of the replacement.

At this time, both Test Loop 1 (Therminol fluid, GA FMSC collector) and Test Loop 3 (high pressure water, Suntec collector) were being operated simultaneously. On 20 October 1977 an electrical short-circuit in Loop 3 caused fluid flow to be lost in that system; in the emergency rush to defocus the Suntec collector and restore fluid flow to Loop 3, it was not noticed for several minutes that flow had also been lost through the GA FMSC collector on Loop 1. The two systems are independent; however, the voltage surge from the short-circuit condition was enough to cause the fluid circulation pump relay to drop out, stopping fluid flow with the FMSC still in full focus.

Loop 3 circulation could not be restored; the pumps on Loop 1 restarted without difficulty when the lack of flow was discovered. Examination of the data printout revealed that flow had been zero for about 12 minutes. Approximately one minute before flow was resumed, skin temperatures measured in the illuminated side of the absorber tube were 532.6, 508.1, and 505.9°C. A plot of one skin temperature thermocouple during this incident is shown in Figure 11. Measured fluid temperatures did not increase to the same extent because the fluid thermocouples were in mixers just off the end of the absorber, and thus not directly exposed to the fluid in direct illumination. The maximum fluid temperature recorded was 332°C.

Examination of the receiver assembly after shutdown showed numerous holes had melted in the Tedlar film across the receiver aperture and the formerly black absorber tube surface was now light tan in color. No overpressure occurred, so the absorber was not physically deformed.

Efficiency and losses were measured the following day after the remnants of the Tedlar window were removed. Temperature and flow conditions identical to those

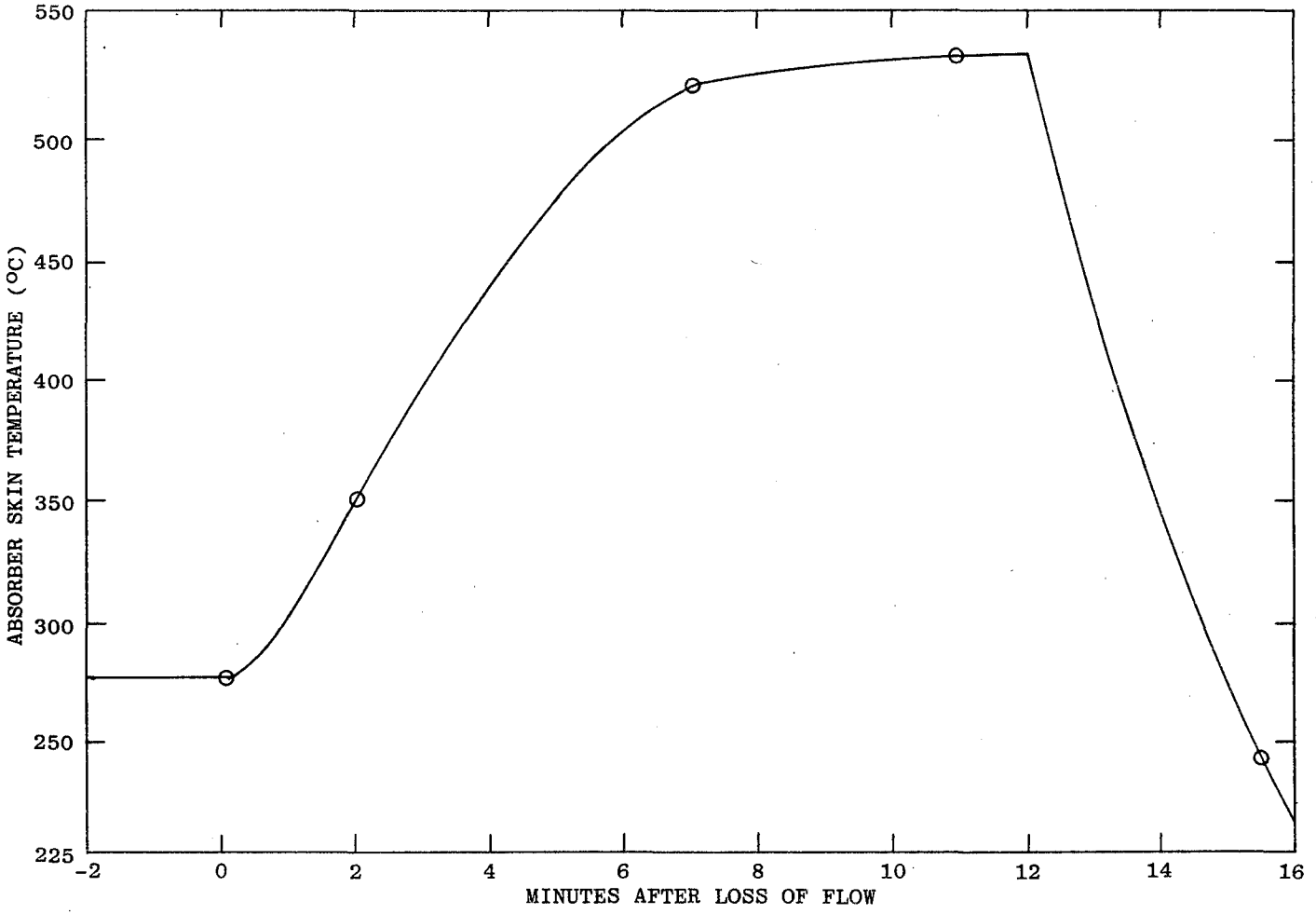

Figure 11. FMSC Absorber Temperatures After Loss of Fluid Flow.

measured prior to the overheat were established. As expected, efficiency had decreased; the 41% efficiency of the previous day was now down to 36% due to reduced absorptance and increased losses.

The absorptance and emissivity of the absorber were not remeasured after this overheat condition occurred. After the first overheat the absorptance had decreased from 0.956 to 0.77 (see Table 2); calculations using the 5% drop in measured efficiency after the second incident indicate that the absorptance was down only about half as much. This magnitude of decrease is consistent with the time the tube was subjected to the high temperature, about 20 minutes the first time and 12 minutes during the second incident.

An extensive series of receiver thermal loss tests was performed. The results were divided into three categories for low, medium and high flow-rates in an attempt to determine any effect of flow-rate on the thermal loss. Tabular data is given in Tables 3, 4, and 5; the same data is plotted in Figures 12, 13, and 14. In each of the figures loss is shown in watts, watts per meter of receiver length, and in watts per meter^2 of collector aperture. The curves are a least-squares fit to the data. Included in the loss data are several data points obtained when there was little or no sunshine, and several taken after the overheat incident had damaged the black chrome surface and removed the receiver window. These data points are plotted in Figures 12, 13, and 14 but were not included in calculating the least-squares curve fit.

Figure 15 is a composite loss plot for comparison of the curves from Figures 12, 13, and 14. This figure indicates a small effect of flow-rate on the thermal loss. It was expected that higher flow-rates, with a more turbulent flow and a slightly higher average receiver temperature, would exhibit higher loss. The opposite was found; the lower flow-rates show the greater losses. One possible explanation is the heat contribution due to friction losses at the higher flow-rates. The high and low flow-rate loss curves in Figure 14 differ by about 100 watts. Converted to pressure drop across the receiver, 100 watts corresponds to about 230 kPa (33 psi). Unfortunately, accurate differential pressure measurements were not made during this test series, however, pressures of approximately this magnitude were observed during the test. Except for this friction heating factor, loss dependance on flow-rate is probably smaller than the scatter in the measured data.

The points labeled "window removed" in Figures 12, 13, and 14 are those obtained after the black chrome was damaged in the overheat incident; the Teflon window was also completely removed for these tests. As expected, the losses were greatly increased. Most of the increase was probably due to conduction and convection losses caused by the missing window.

Figure 16 shows the positions and relative spacing of the six mirror segments and the five measurement points on the receiver assembly used to obtain focal line intensity scan data. Table 6 identifies the various scan positions with the input conditions and the figure in which the data is plotted. Figures 17 through 21 contain the scan intensity data obtained on the five measurement locations on the receiver. In each figure the apparent secondary aperture width is also shown to illustrate the magnitude of the light lost. It is immediately obvious from Figures 17-21 that some mirror segments produced a good image at the receiver, so

Table 3. Receiver Heat Loss at High Flow Rates.

Test Date	Input Temp (°C)	Receiver ΔT (°C)	Flow (Liters/min)	Loss (kJ/hr)	Wind (m/sec)	Ambient Temp (°C)	Solar Input (W/m^2)
8/16/77	176.3	0.7	19.94	1809	1.2	23.8	832
8/17/77	102.5	0.3	18.8	725	1.2	22.2	867
8/17/77	262.1	1.7	18.8	3952	2.1	30.0	400
8/17/77	103.0	0.3	23.9	755	1.4	22.7	867
8/22/77	175.2	0.6	18.6	1297	0.8	29.4	924
8/22/77	176.3	0.3	26.1	872	1.9	28.3	933
8/23/77	246.7	1.1	18.4	2479	3.4	31.6	936
8/23/77	247.2	0.6	24.8	1785	0.8	30.0	939
8/24/77	303.9	1.7	18.6	3942	1.3	30.5	889
8/26/77	242.1	1.2	18.4	2761	2.4	31.1	977
8/29/77	176.3	1.0	19.2	1643	3.6	31.1	908
8/30/77	307.0	1.8	19.5	4460	2.1	24.4	0*
8/30/77	307.3	1.9	34.4	5119	2.8	27.7	3
8/31/77	308.3	1.8	19.4	4423	1.3	28.8	883
9/21/77	246.6	1.5	19.0	3548	1.9	25.5	1002
9/21/77	247.1	0.8	26.6	2999	2.1	24.4	1015
9/22/77	243.6	1.4	27.8	5193	0	25.0	1.6†
9/23/77	175.4	1.1	25.5	2867	2.4	22.0	753†

*Light rain, dark clouds
†Mylar window removed, black chrome damaged

Table 4. Receiver Heat Loss at Medium Flow Rates.

Test Date	Input Temp (°C)	Receiver ΔT (°C)	Flow (Liters/min)	Loss (kJ/hr)	Wind (m/sec)	Ambient Temp (°C)	Solar Input (W/m^2)
8/16/77	175.5	1.2	10.7	1554	1.2	26.6	832
8/17/77	104.6	0.6	12.0	782	1.6	25.0	867
8/18/77	305.3	3.6	12.0	5218	2.0	27.7	902
8/18/77	198.2	1.3	15.2	2161	0.9	21.6	66
8/22/77	175.3	0.9	11.6	1198	1.0	26.6	9
8/17/77	260.3	2.9	11.5	3562	2.3	30.0	438
8/23/77	245.5	2.2	11.5	2321	3.4	31.1	927
8/24/77	298.2	3.3	11.2	3805	1.1	30.0	889
8/30/77	304.2	3.5	11.2	4953	2.6	25.5	6
8/31/77	305.8	3.4	11.2	4463	2.0	28.8	848
9/16/77	241.7	2.4	14.2	4199	1.0	26.1	19
9/22/77	246.2	3.8	11.1	5354	1.8	23.8	6*

*Mylar window removed, black chrome damaged

that most of the focused light could be captured by the receiver; for example, see Figure 19. Other segments produced a fairly poor image, as seen in Figure 21.

Some of the results of an analysis of the near noon scan data by General Atomic are shown in Table 7 (data from Reference 6), indicating that only about 71% of the reflected light was captured by the receiver.

By contrast, preliminary results of scan testing on several new FMSC modules being installed in the Midtemperature Solar Systems Test Facility show about 90% of the reflected light is being captured.

Table 5. Receiver Heat Loss at Low Flow Rates.

Test Date	Input Temp (°C)	Receiver ΔT (°C)	Flow (Liters/min)	Loss (kJ/hr)	Wind (m/sec)	Ambient Temp (°C)	Solar Input (W/m^2)
8/16/77	169.3	5.2	3.06	1695.6	2.1	26.6	832
8/17/77	104.2	1.3	4.3	662.8	0.5	23.8	867
8/17/77	255.3	7.2	4.1	3535	1.6	30.5	738
8/18/77	296.7	10.00	3.7	4462	2.2	27.7	895
8/22/77	175.7	2.6	4.8	1330	1.7	25.0	9
8/23/77	240.6	5.8	3.7	2580	1.4	31.1	898
8/24/77	290.2	10.1	3.1	3682	1.4	31.1	889
8/26/77	234.6	6.4	4.1	3115	2.6	31.6	971
8/30/77	294.4	11.0	3.5	4561	3.6	21.6	0*
9/21/77	243.9	8.5	3.4	3512	1.7	25.5	980
9/22/77	242.7	11.1	3.8	4900	0.2	25.5	28†

*Light rain falling during measurement; dark clouds
†Mylar window removed. Black chrome heavily damaged

Table 6. Identification of Focal Line Intensity Scans.

Test Position*	Test Date	Solar Time	Solar Insolation (W/m^2)	Curve Number	Figure Number
1	9/10/77	11:50	993	1	17
1	9/10/77	13:25	905	2	17
1	9/10/77	15:12	804	3	17
2	9/04/77	12:43	905	1	18
3	9/04/77	11:12	917	1	19
4	9/04/77	10:52	902	1	20
4	9/04/77	12:09	911	2	20
5	9/11/77	11:32	999	1	21
5	9/11/77	8:50	914	2	21
5	9/11/77	12:30	914	3	21
5	9/11/77	7:52	615	4	21

*See Figure 16 for test position locations.

Table 7. Light Collection Efficiency*.

Position	Solar Time	Light Collection Efficiency
1	11:50	63.0%
2	12:43	79.1%
3	11:12	81.5%
4	12:09	65.6%
5	12:30	67.3%

*Average = 71.3% ±8.4%

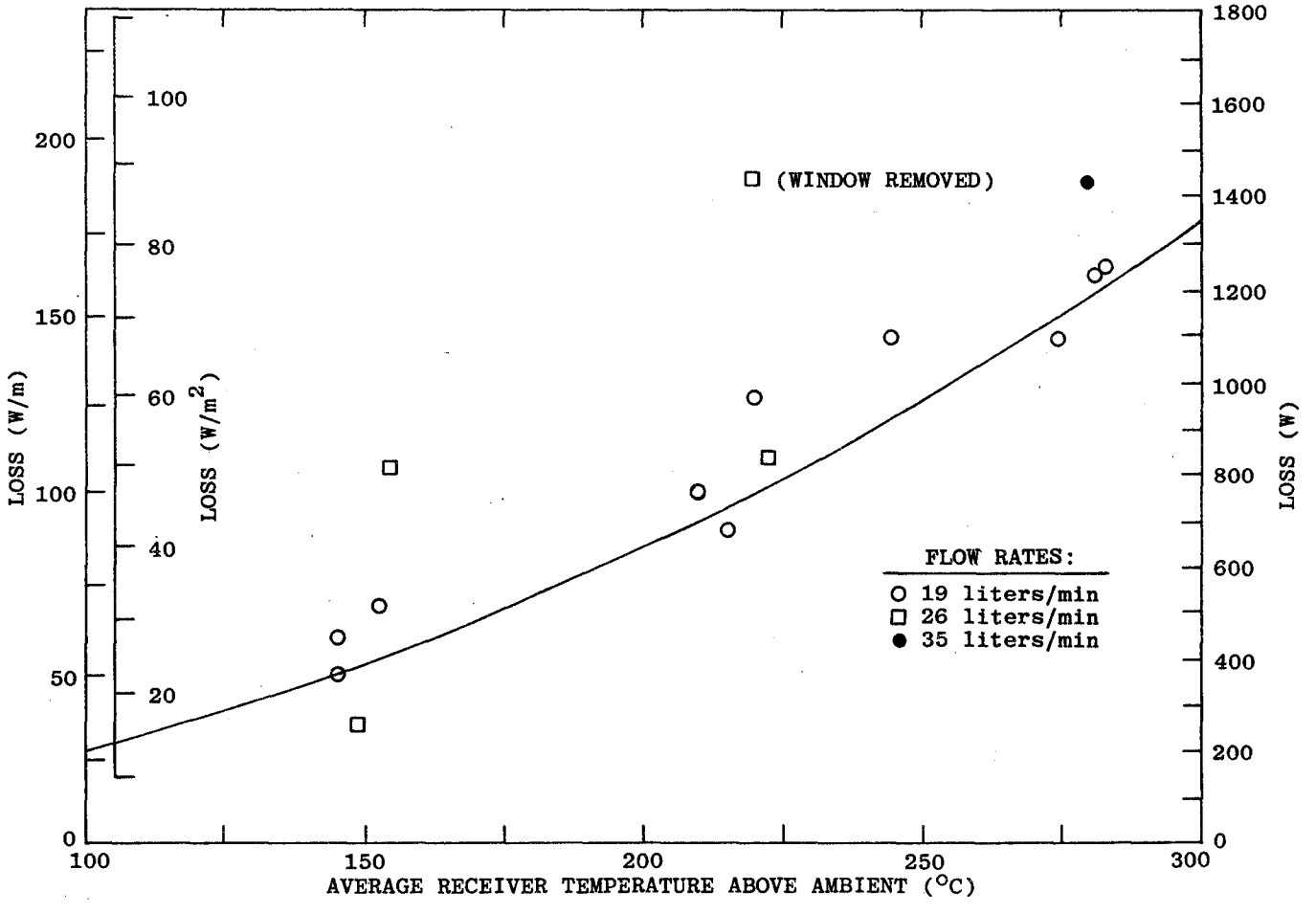

Figure 12. FMSC Receiver Loss at High Flow Rates.

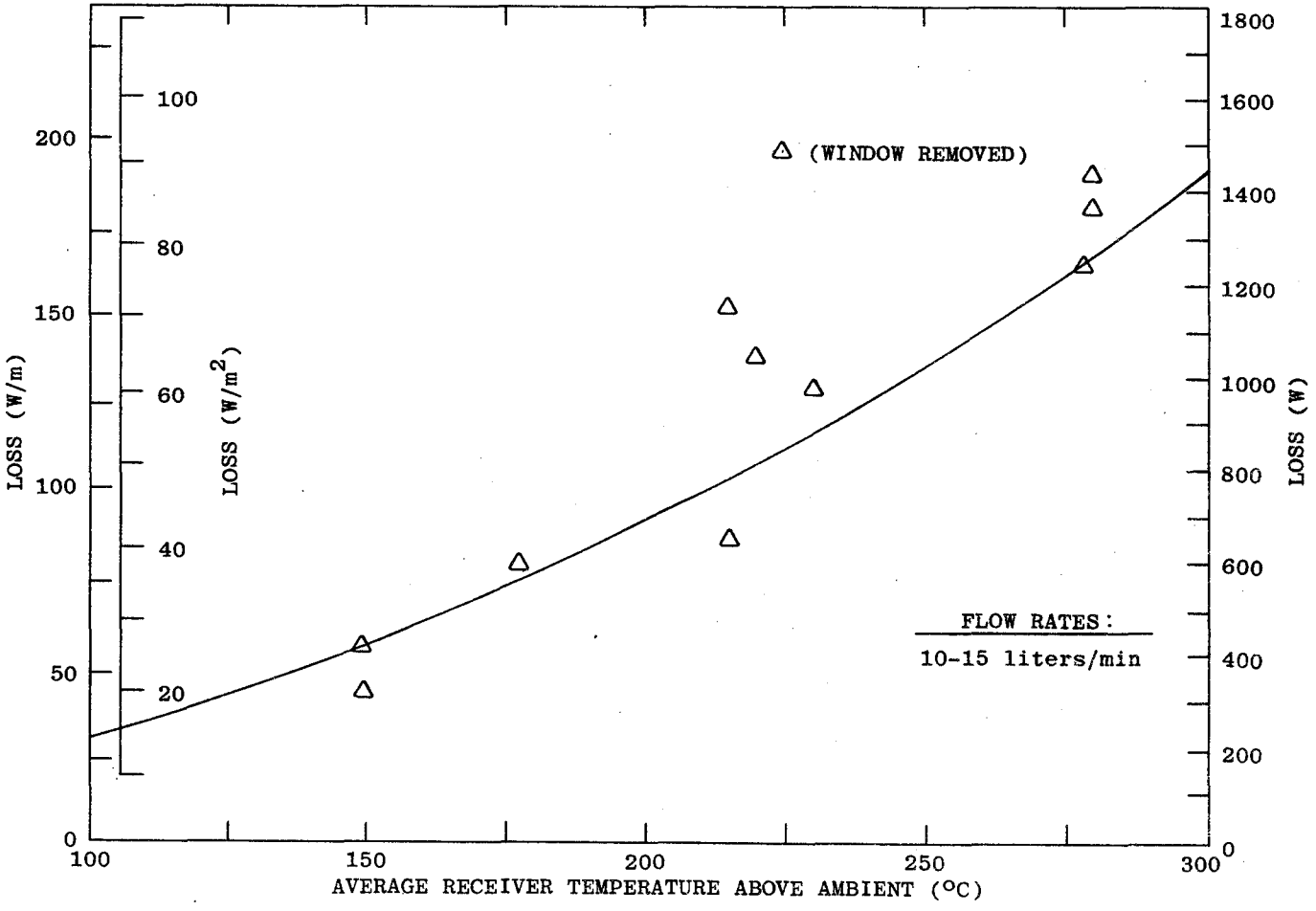

Figure 13. FMSC Receiver Loss at Medium Flow Rates.

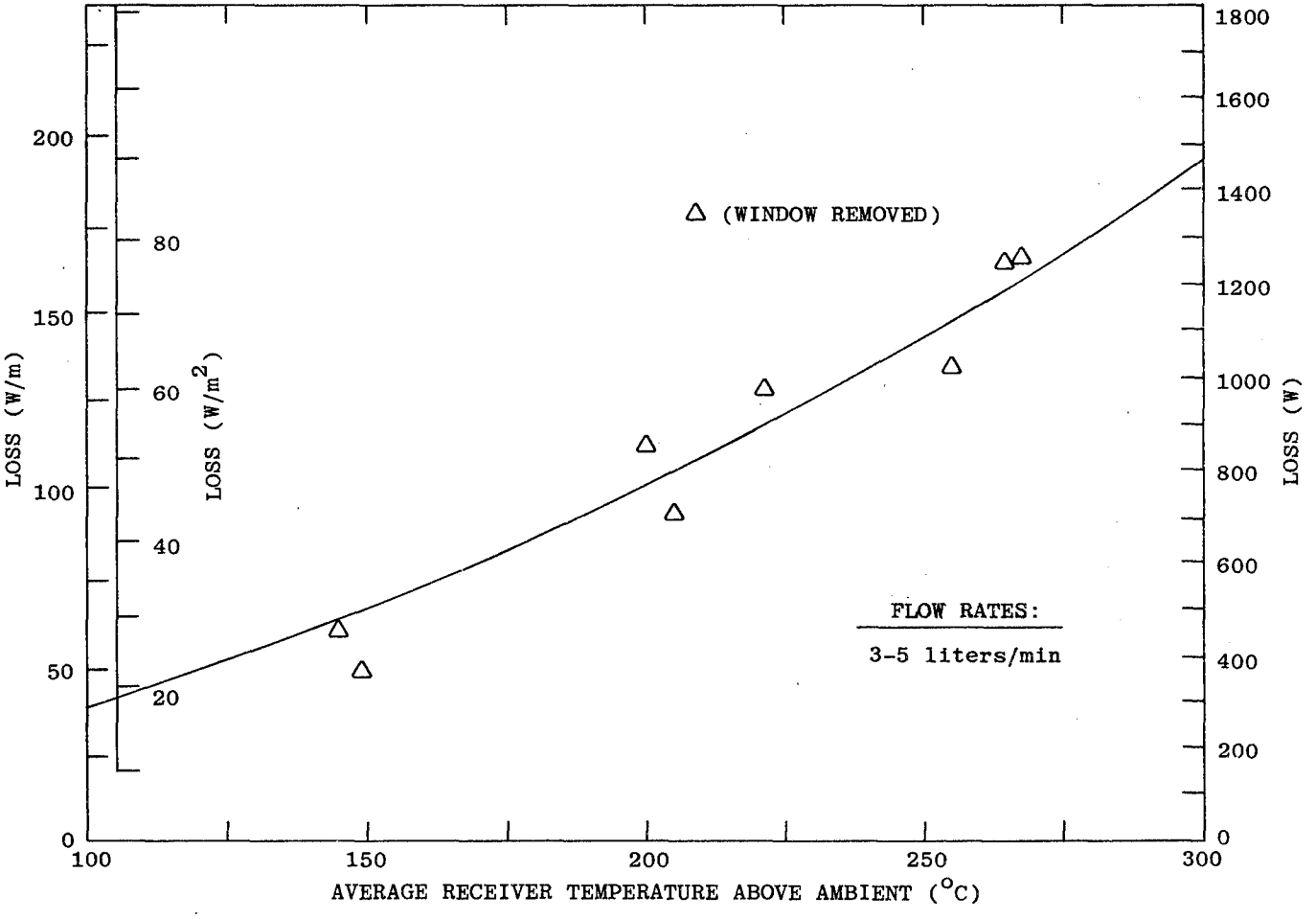

Figure 14. FMSC Receiver Loss at Low Flow Rates.

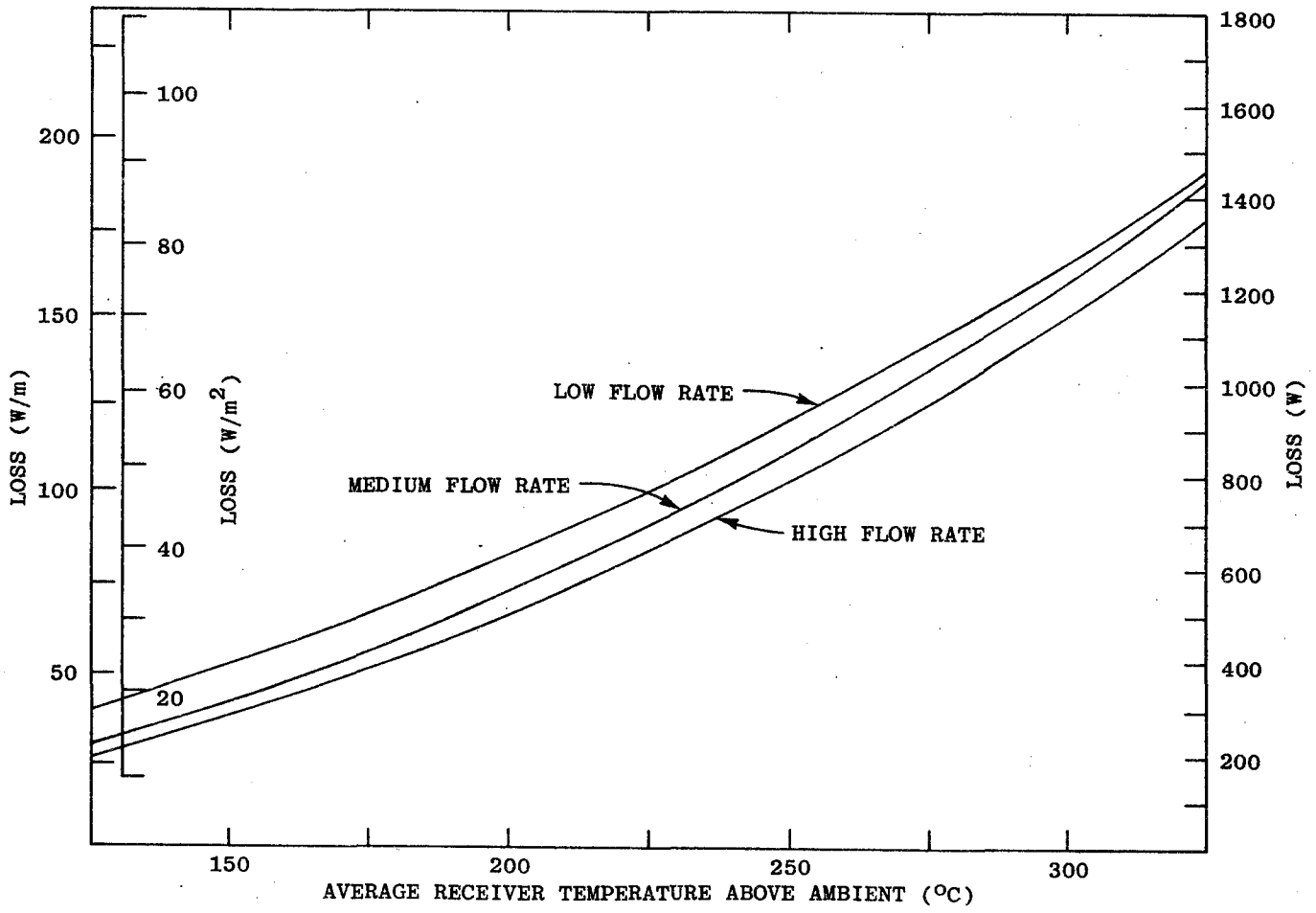

Figure 15. FMSC Thermal Loss.

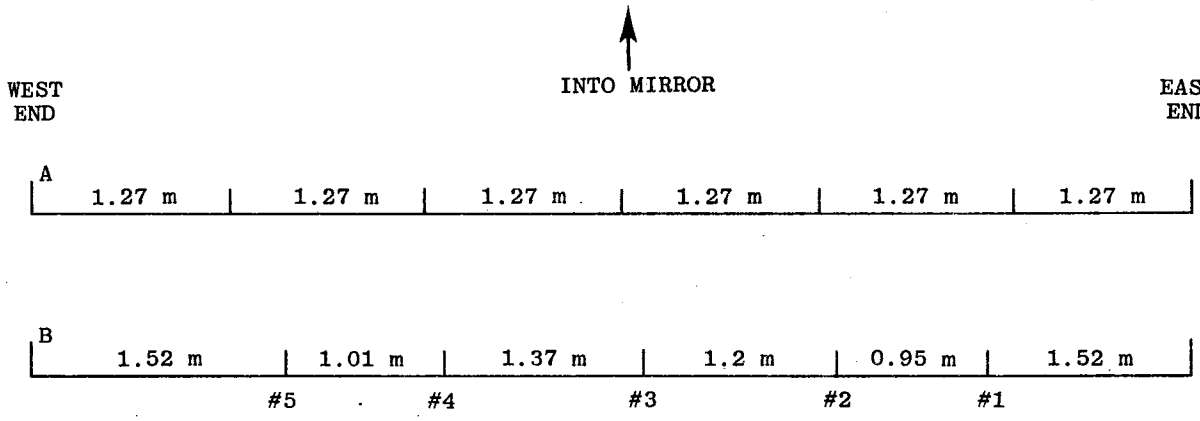

A. Mirror module configuration showing the 1.27 m mirror segments.

B. The measurement profile showing the location of the measurement points and the distances between them. No. 1 is on the East end and No. 5 is on the West end.

Figure 16. Solar Cell Measurement Points with Respect to Mirror Segment Location.

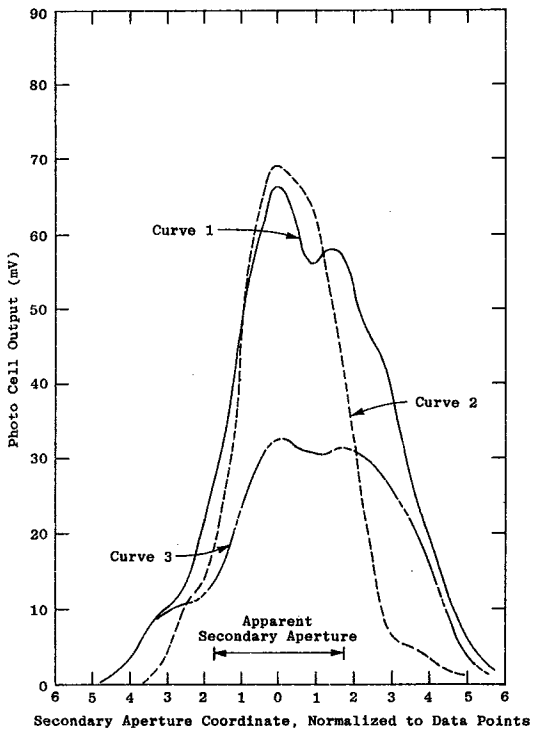

Figure 17. Focal Line Intensity Scans at Position 1.

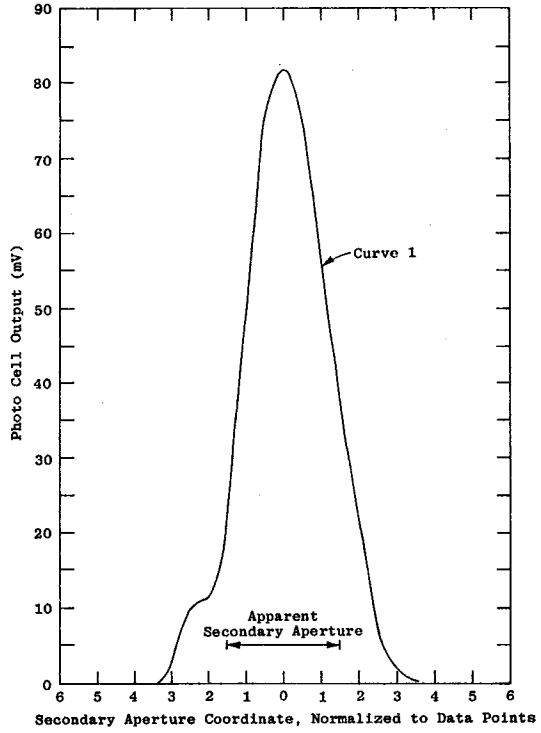

Figure 18. Focal Line Intensity Scans at Position 2.

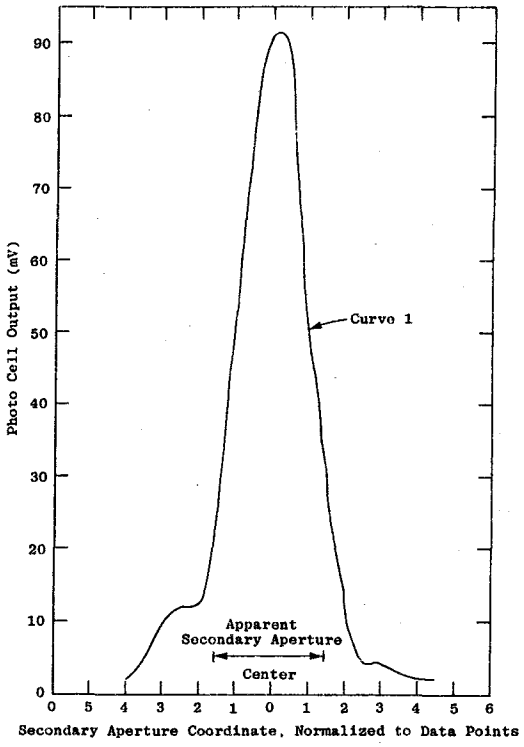

Figure 19. Focal Line Intensity Scans at Position 3.

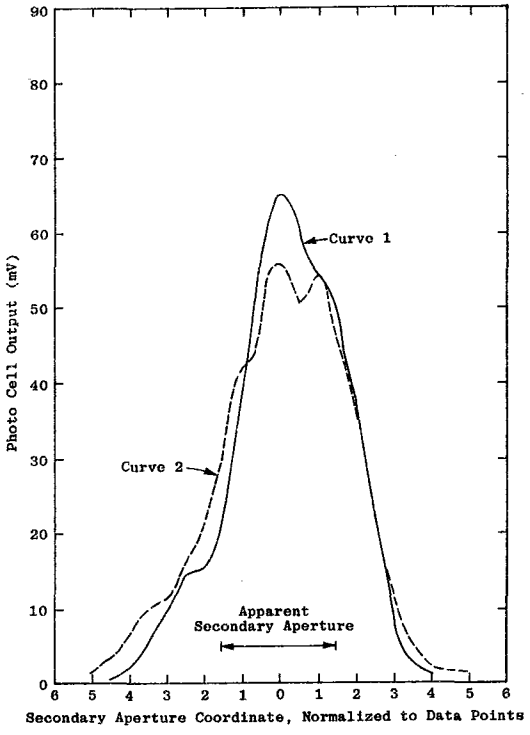

Figure 20. Focal Line Intensity Scans at Position 4.

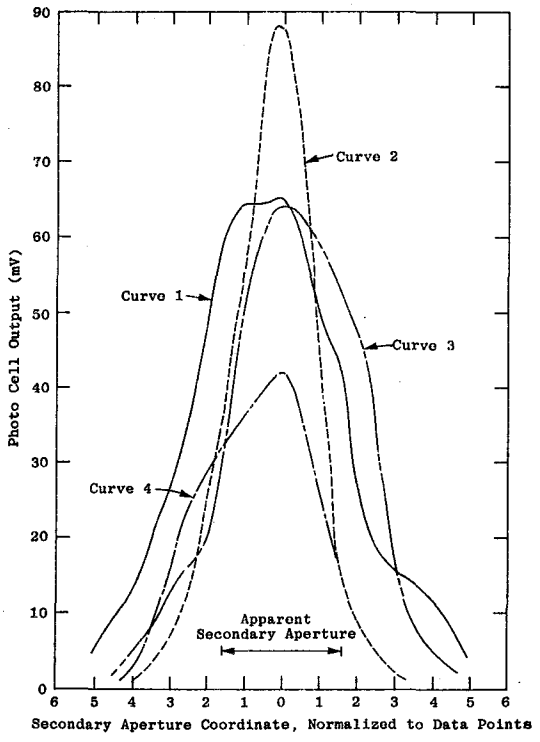

Figure 21. Focal Line Intensity Scans at Position 5.

SUMMARY OF RESULTS AND CONCLUSIONS: The General Atomic FMSC modules produced disappointing results during their efficiency testing. The peak efficiency near 300°C was expected to be about 50%; the measured peak efficiency was about 42%. Reasons for this are readily identified. The dominant deficiency was loss of about 30% of the reflected light because of poor focus. In turn, the lack of a sharp focal line can be traced to variations in positions of the individual mirror segments. Several reasons are possible for the mirrors not being precisely placed. The most important are: 1) the form used for casting the concrete module may not have been rigid enough, leading to some deformation of the structure, 2) chipping of edges and facet surfaces when removing concrete form added grit and irregularities which could cause individual mirrors to be randomly out of focus--a condition which was observed on the test modules, 3) the test modules had new replacement mirrors temporarily installed without a complete bond to the module over their entire rear surface. This was done so that the mirrors could be removed for use in the larger field, but late in the test series it was observed that the mirrors were not all lying flat on their underlying facets. Assuming that the concrete facets were sufficiently precise (not a known fact), additional adhesive on the individual replacement mirror segments would have improved the focus. Most of these deficiencies would be easily correctable in building a new system based on the FMSC modules.

Preliminary tests on the new FMSC modules have indicated that the first two of these difficulties have been reduced to acceptable levels and the third was the result of a temporary measure which would not be expected in a permanent installation.

If 100% of the light from the mirror surface had been captured by the receiver, the thermal efficiency would have been about 62% at 300°C. The 90% capture demonstrated by a preliminary test on a module installed in the systems test facility would have produced an efficiency of about 53% at 300°C, a notable improvement over the 42.5% actually measured with the test modules.

The thermal loss measured on the FMSC receiver was very low; the loss per unit length of receiver was among the lowest achieved by any of the collectors tested at the CMTF. The exceptionally low conductivity of the Microtherm insulation and secondary concentration to a smaller active receiver are probably the primary reasons for the low loss rate. The window was also important, as can be seen from the dramatic increase in loss when the window was removed.

In summary, this evaluation has shown the thermal performance of the General Atomic Fixed Mirror Solar Concentrator to be lower than expected. However, the deficiencies have been identified as being caused by problems which can be corrected in the manufacturing process for future modules produced by General Atomic.

References

1. Sandia Laboratories, "Solar Total Energy Program Plan," SAND76-0167 (Revised), August 1976.

2. J. L. Russell, Jr., E. P. DePlomb, and R. K. Bansal, "Principles of the Fixed Mirror Solar Concentrator," General Atomic Company Report GA-A12902, May 31, 1974.

3. J. L. Russell, Jr., J. R. Schuster, and G. H. Eggers, "Development Status of the Fixed Mirror Solar Concentrator," General Atomic Company Report GA-A14375, June 1977.

4. G. H. Eggers, "Performance of the FMSC Test Modules," Final Report, Contract 05-6121, General Atomic Company, February 1978.

5. Monsanto Company, Therminol 66, Technical Data Sheet, IC/FF-35.

6. T. Harrison, W. Dworzak, and C. Folkner, "Solar Collector Module Test Facility, Instrumentation Fluid Loop Number One," Sandia Laboratories Report SAND76-0425, January 1977.

DISTRIBUTION:
TID-4500-R66, UC-62 (316)

Aerospace Corporation
P.O. Box 92957
Los Angeles, CA 90009
Attn: Richard Bruce

Aerospace Corporation
2350 E. El Segundo Blvd.
El Segundo, CA 90245
Attn: Leon Bush

Aerospace Corporation
101 Continental Blvd.
El Segundo, CA 90245
Attn: Elliott L. Katz

Acurex Aerotherm
485 Clyde Avenue
Mountain View, CA 94042
Attn: G. J. Neuner

American Gas Association
1515 Wilson Boulevard
Arlington, VA 22209
Attn: P. Susey

Solar Total Energy Program
American Technological University
P.O. Box 1416
Killeen, TX 76541
Attn: John J. Kincel, Director

Argonne National Laboratory (3)
9700 South Cass Avenue
Argonne, IL 60439
Attn: R. G. Matlock
W. W. Schertz
Roland Winston

Atlantic Richfield Co.
515 South Flower Street
Los Angeles, CA 90071
Attn: H. R. Blieden

Barber Nichols Engineering
6325 W. 55th Avenue
Arvada, CO 80002
Attn: R. G. Olander

Battelle Memorial Institute
Pacific Northwest Laboratory
P.O. Box 999
Richland, WA 99352
Attn: K. Drumheller

Brookhaven National Laboratory
Associated Universities, Inc.
Upton, LI, NY 11973
Attn: J. Blewett

Congressional Research Service
Library of Congress
Washington, DC 20540
Attn: H. Bullis

Del Manufacturing Co.
905 Monterey Pass Road
Monterey Park, CA 91754
Attn: M. M. Delgado

Desert Research Institute
Energy Systems Laboratory
1500 Buchanan Blvd.
Boulder City, NV 89005
Attn: Jerry O. Bradley

Desert Sunshine Exposure Inc.
P.O. Box 185
Phoenix, AZ 85020
Attn: Gene A. Zerlaut

Honorable Pete V. Domenici
Room 405
Russell Senate Office Bldg.
Washington, DC 20510

Edison Electric Institute
90 Park Avenue
New York, NY 10016
Attn: L. O. Elsaesser,
Director of Research

Energy Institute
1700 Las Lomas
Albuquerque, NM 87131
Attn: T. T. Shishman

EPRI
3412 Hillview Avenue
Palo Alto, CA 94303
Attn: J. E. Bigger

General Atomic
P.O. Box 81608
San Diego, CA 92138
Attn: G. Eggers

General Electric Company
Valley Forge Space Center
Valley Forge, PA 19087
Attn: Walt Pijawka

General Electric Co.
P.O. Box 8661
Philadelphia, PA 19101
Attn: A. J. Poche

Georgia Institute of Technology
American Society of Mechanical
Engineers
Atlanta, GA 30332
Attn: S. Peter Kezios, President

DISTRIBUTION (cont)
Georgia Power Company
Atlanta, GA 30302
Attn: Mr. Walter Hensley
Vice President Economics Services

Grumman Corporation
4175 Veterans Memorial Highway
Ronkonkoma, NY 11779
Attn: Ed Diamond

Hexcel
11711 Dublin Blvd.
Dublin, CA 94566
Attn: George P. Branch

Jet Propulsion Laboratory
Bldg. 277, Rm. 201
4800 Oak Grove Drive
Pasadena, CA 91103
Attn: V. C. Truscello

Lawrence Berkley Laboratory
University of California
Berkley, CA 94720
Attn: Mike Wallig

Lawrence Livermore Laboratory
University of California
P.O. Box 808
Livermore, CA 94500
Attn: W. C. Dickinson

Los Alamos Scientific Laboratory (2)
Los Alamos, NM 87545
Attn: J. D. Balcomb
MS 571 Q-DO
D. P. Grimmer
MS Q-11, Solar Group

Honorable Manuel Lujan
1323 Longworth Building
Washington, DC 20515

Mann-Russell Electronics, Inc.
1401 Thorne Road
Tacoma, WA 98421
Attn: G. F. Russell

Martin Marietta Aerospace
P.O. Box 179
Denver, CO 80201
Attn: R. C. Rozycki

McDonnell-Douglas Astronautics Co.
5301 Bolsa Avenue
Huntington Beach, CA 92647
Attn: Don Steinmeyer

NASA-Lewis Research Center
Cleveland, OH 44135
Attn: R. Hyland

New Mexico State University
Las Cruces, NM 88001
Attn: R. L. San Martin

Oak Ridge Associated Universities
P.O. Box 117
Oak Ridge, TN 37830
Attn: A. Roy

Oak Ridge National Laboratory
P.O. Box Y
Oak Ridge, TN 37830
Attn: J. R. Blevins
J. Johnson
S. I. Kaplan
R. Pearlstein

Office of Science and Technology
Executive Office of the President
Washington, DC 20506
Attn: R. Balzhizer

Office of Technology Assessment
Old Immigration Building, Rm 722
119 D. Street, NE
Washington, DC 20002

Omnium G
1815 Orangethorpe Park
Anaheim, CA 92801
Attn: Ron Derby
S. P. Lazzara

Rocket Research Company
York Center
Redmond, WA 98052
Attn: R. J. Stryer

Honorable Harold Runnels
1535 Longworth Building
Washington, DC 20515

Honorable Harrison H. Schmitt
Room 1251
Dirksen Senate Office Bldg.
Washington, DC 20510

Scientific Atlanta, Inc.
3845 Pleasantdale Road
Atlanta, Georgia 30340
Attn: Andrew L. Blackshaw

Sensor Technology, Inc.
21012 Lassen Street
Chatsworth, CA 91311
Attn: Irwin Rubin

Solar Energy Research Institute
1536 Cole Blvd
Golden, CO 80401
Attn: C. J. Bishop
Ken Brown
B. L. Butler
Frank Kreith
Charles Grosskreutz
B. P. Gupta

DISTRIBUTION (cont)
Solar Energy Technology
Rocketdyne Division
6633 Canoca Avenue
Canoca Park, CA 91304
Attn: J. M. Friefeld

Solar Kinetics Inc.
P.O. Box 10764
Dallas, TX 75207
Attn: Gus Hutchison

Southwest Research Institute
P.O. Box 28510
San Antonio, TX 78284
Attn: Danny M. Deffenbaugh

Stanford Research Institute
Menlo Park, CA 94025
Attn: Arthur J. Slemmons

Stone & Webster
Box 5406
Denver, CO 80217
Attn: V. O. Staub

Sun Gas Company
Suite 800, 2 No. Pk. E
Dallas, TX 75231
Attn: R. C. Clark

Sundstrand Electric Power
4747 Harrison Avenue
Rockford, IL 61101
Attn: A. W. Adam

Suntec Systems Inc.
21405 Hamburg Avenue
Lakeville, MN 55044
Attn: J. H. Davison

Swedlow, Inc.
12122 Western Avenue
Garden Grove, CA 92645
Attn: E. Nixon

TEAM Inc,
8136 Old Keene Mill Road
Springfield, VA 22152
Attn: Daniel Ahearne

Tennessee Energy Office
Suite 250, Capitol Hill Bldg.
Nashville, TN 37219
Attn: Carroll V. Kroeger, Sr.

U.S. Department of Energy
Agricultural & Industrial
Process Heat
Conservation & Solar Application
MS 2221C
20 Massachusetts Avenue NW
Washington, DC 20545
Attn: W. W. Auer

U.S. Department of Energy (3)
Albuquerque Operationis Office
P.O. Box 5400
Albuquerque, NM 87185
Attn: D. K. Nowlin
G. W. Rhodes
J. R. Roder

U.S. Department of Energy
Division of Energy Storage
Systems
4th Floor, RM 416
600 E Streety
Washington, DC 20545

U.S. Department of Energy (9)
Division of Solar Energy
Washington, DC 20545
Attn: R. H. Annan
G. W. Braun
M. U. Gutstein
G. M. Kaplan
H. H. Marvin
Lou Melamed
J. E. Rannels
M. E. Resner
J. Weisiger

U.S. Department of Energy
Los Angeles Operations Office
350 S. Figueroa Street, Suite 285
Los Angeles, CA 90071
Attn: Fred A. Glaski

U.S. Department of Energy
San Francisco Operations Office
1333 Broadway, Wells Fargo Bldg.
Oakland, CA 94612
Attn: Jack Blasy

U.S. Department of Interior
Room 5204
Washington, DC 20204
Attn: M. Prochnik

University of Arkansas
Mechanical Engineering Dept.
Fayetteville, AR 72701
Attn: Dr. F. K. Deaver

University of Delaware
Institute of Energy Conversiuon
Newark, DE 19711
Attn: K. W. Boer

University of New Mexico (2)
Department of Mechanical Eng.
Albuquerque, NM 87113
Attn: W. A. Cross
M. W. Wilden

DISTRIBUTION (cont)
Watt Engineering Ltd.
RR1, Box 183 1/2
Cedaredge, CO 81413
Attn: A. D. Watt

Western Control Systems
13640 Silver Lake Drive
Poway, CA 92064
Attn: L. P. Cappiello

Westinghouse Electric Corp.
P.O. Box 10864
Pittsburgh, PA 15236
Attn: J. Buggy

1100 C. D. Broyles
1260 K. J. Touryan
1262 H. C. Hardee
1280 T. B. Lane
1284 R. T. Othmer
1300 D. B. Shuster
1330 R. C. Maydew
2300 J. C. King
2320 K. L. Gillespie
2323 C. M. Gabriel
2324 L. W. Schulz
2326 G. M. Heck
3161 J. E. Mitchell
3700 L. S. Conterno
5000 A. Narath
5200 E. H. Beckner
5231 J. H. Renken
5700 J. H. Scott
5710 G. E. Brandvold
5711 J. F. Banas
5712 J. A. Leonard
5713 B. W. Marshall
5714 R. P. Stromberg
5715 R. H. Braasch
5719 D. G. Schueler
5730 H. M. Stoller
5740 V. L. Dugan
5800 R. S. Claassen
Attn: R. G. Kepler, 5810
R. L. Schwoebel, 5820
5830 M. J. Davis
5831 N. J. Magnani
5834 D. M. Mattox
5840 H. J. Saxton
5842 J. N. Sweet
5844 F. P. Gerstle
5846 E. K. Beauchamp
8100 L. Gutierrez
8130 R. C. Wayne
8131 W. G. Wilson
8132 A. C. Skinrood
8266 E. A. Aas
8313 R. W. Mar
9330 A. J. Clark, Jr.
9340 W. E. Caldes
9350 F. W. Neilson
9352 O. N. Burchett
9400 H. E. Lenander
9572 L. G. Rainhart
9700 R. E. Hopper
Attn: H. H. Pastorius, 9740
R. W. Hunnicutt, 9750
3141 C. A. Pepmueller (5)
3151 W. L. Garner (3)
For DOE/TIC
(Unlimited Release)
6011 G. C. Newlin